Materials Characterization 144 (2018) 42–47

Contents lists available at ScienceDirect

Materials Characterization

journal homepage: www.elsevier.com/locate/matchar

High elongation achieved by band-like distribution of reinforcements in aluminum matrix composites

Kesong Miao[a], Danyang Li[a], Guangze Tang[a,*], Chao Xu[a], Lin Geng[a], Jie Zhang[a], Xuesong Leng[a], Huijun Kang[b], Tongmin Wang[b], Shuai Yan[c], Honglan Xie[c], Tiqiao Xiao[c], Guohua Fan[a,d,**]

[a] School of Materials Science and Engineering, Harbin Institute of Technology, Harbin 150001, PR China
[b] School of Materials Science and Engineering, Dalian University of Technology, Dalian 116000, PR China
[c] Shanghai Synchrotron Radiation Facility, Shanghai 201204, PR China
[d] Key Laboratory of Micro-systems and Micro-structures Manufacturing of Ministry of Education, Harbin Institute of Technology, Harbin 150001, PR China

ARTICLE INFO

Keywords:
Whisker reinforced composites
Residual stress
Plastic deformation
Fracture
Band-like distribution

ABSTRACT

Ductile aluminum matrix composites reinforced by $Al_{18}B_4O_{33}$ whisker (ABO) with band-like distribution (Band-like Aluminum Matrix Composites, BAMCs) were fabricated by powder metallurgy and extrusion followed by annealing. The cracks tend to nucleate in the ABO-rich bands, but the band-like structure induces compressive residual stress then suppresses the crack propagation and improves the strain transferring ability in the BAMCs. The denser and smaller cracks formed in the BAMCs with higher ABO volume fraction during tensile test. These cracks play an important role in the strain non-localization process, but have negligible contribution to the tensile strain.

1. Introduction

Aluminum matrix composites (AMCs) have a lot of advantages, such as high specific strength and stiffness, low thermal expansion and superior damping capabilities [1–3]. However, the reinforcement agglomeration deteriorates the ductility of the AMCs [4–6]. The drastic drop of ductility in the AMCs with increasing reinforcement content results in poor safety and formability, which limits their application. It is reported that the materials involving structural architectures such as bi-continuous [7], layered [8–11] and gradient structures [12] achieve excellent strength-ductility balance. Huang et al. [10] reported that the layered structure relieves the strain localization and remarkably improves the tensile ductility of the Ti/Al metal composites. Since the ductility of AMCs also strongly depends on the plastic strain localization behaviour [13], strain partitioning adjustment by structural architecture should be a potential way to improve the poor ductility of AMCs with high reinforcement content.

In this work, the band-like aluminum matrix composites (BAMCs) with the nominal $Al_{18}B_4O_{33}$ whisker (ABO) volume fraction (V_w) of 3%, 5% and 10% were fabricated and they are denoted as 3ABO, 5ABO and 10ABO, respectively. The microstructure of the BAMCs comprises the ABO-rich bands and the surrounding ABO-poor regions and accordingly, high elongation was obtained. In order to investigate the effect of band-like distribution of ABO on the deformation behaviour in the BAMCs, the contribution of the plastic strain (ε_p) and the crack strain (ε_c) were quantitatively measured by digital image correlation (DIC) and synchrotron X-ray tomography, respectively.

2. Materials and Methods

The BAMCs were fabricated by the following steps: the pure Al powder (48 μm in diameter) was blended with ABO (1.7 μm in diameter and 30 μm in length) by the V_w of 3%, 5% and 10%. The ball-to-powder weight ratio (4: 1), speed of ball milling (140 rpm) and milling time (4.0 h) were used in the blending. The details of materials before and after blending could be found in Supplementary information (SI). The as-mixed powders were hot-pressing sintered at 25 MPa and 640 °C for 1 h, followed by furnace cooling. The as-sintered composites were extruded at 450 °C with an extrusion ratio of 25: 1 and then, the as-extruded composites were annealed at 400 °C for 1 h, followed by furnace cooling. The microstructure of the BAMCs was observed by scanning electron microscope (SEM, HELIOS NanoLab 600i) equipped with an electron backscattering diffraction (EBSD) system. The specimens for EBSD analysis were electro-polished in the solution of 90 vol% CH_3CH_2OH and 10 vol% $HClO_4$ on the condition of 0.7 A for 10 s. The dog-bone shaped specimens for tensile test were cut from the BAMCs

* Corresponding author.
** Correspondence to: G. Fan, School of Materials Science and Engineering, Harbin Institute of Technology, Harbin 150001, PR China.
E-mail addresses: oaktang@hit.edu.cn (G. Tang), ghfan@hit.edu.cn (G. Fan).

https://doi.org/10.1016/j.matchar.2018.06.031
Received 26 February 2018; Received in revised form 14 June 2018; Accepted 27 June 2018
Available online 02 July 2018
1044-5803/

with the longitudinal axis parallel to the extrusion direction (ED). The gauge length is 15 mm and the cross sectional area is 2 mm × 2.5 mm. The tensile test was conducted using INSTRON-5569 at room temperature (RT). DIC coupled in-situ tensile test was utilized to track the strain (ε) and strain distribution with the combination of optical microscope (OM, Olympus SZX16) and Tensile/Compress Model (Kammrath & Weiss) for large area, SEM and SEM tester 1000 EBSD (MTI) for local area, respectively. It is worthy to note that the resolution of DIC is closely related to the field of view (magnification) of image and the resolution of detector. In the case of DIC based on OM, the magnification is 16× and the resolution of detector is 2560 × 1920, the corresponding resolution is about 2.29 μm. In the case of DIC based on SEM, the magnification is 500× and the resolution of detector is 1024 × 943, the corresponding resolution is about 0.58 μm. The images were captured at the interval of 0.5% true strain under a loading speed of 5 μm/s. The cracks in the fractured tensile specimens were characterized and quantitatively measured by using synchrotron X-ray tomography on the beamline station BL13W1 in Shanghai Synchrotron Radiation Facility (SSRF). The energy of X-ray (18 keV), exposure time (2.0 s) and the resolution of synchrotron X-ray tomography (0.65 μm) were used in this study. The specimens for X-ray tomography were extracted from the centre of the tensile fractured specimen with 1 mm in diameter. The residual stresses were experimentally measured by micro X-ray grazing-incidence diffraction with a 3 μm beam size on beamline station BL15U1, SSRF and Fit-2D software. The details of this experiment are illustrated in SI.

3. Results and Discussion

3.1. The Mechanical Properties and Microstructures of the BAMCs

Fig. 1a–c shows the secondary electron micrographs of the BAMCs. No significant morphology change of single whisker with volume fraction was observed. The ABO (white contrast) distributes heterogeneously in the aluminum matrix (grey contrast), so that the BAMCs comprise the ABO-rich bands that surrounded by ABO-poor regions. The long axis of ABO-rich bands is approximately parallel to ED. This feature is the redistribution effect of extrusion on clusters in as-sintered composites. The ABO-rich bands are refined with as the V_w increases. After the ball milling and extrusion, most of ABOs are broken and the length-diameter ratio of ABO decreases from 17: 1 to about 6.8: 1 [14]. EBSD analysis was carried on the 10ABO with the hit-rate of 68.22% as shown in Fig. 1d. Based on the EBSD result, the 10ABO composite was fully recrystallized after annealing, with a mean grain size of 5.3 μm. Fig. 1e shows the nominal tensile stress-strain curves of the BAMCs. The elongation to failure (ε_T) and the tensile yield strength (σ_{TYS}) of the BAMCs developed in present study and the AMCs that were previously reported are summarized in Fig. 1f for comparison [2, 15–17]. It can be seen that the BAMCs developed in present study exhibit much superior ε_T than the AMCs previously reported, despite of their relatively lower σ_{TYS}. The detailed comparison could be found in Table S1. It is obvious that the BAMCs maintain the superior ε_T even with the increasing V_w rather than the drastic drop of ε_T in the other AMCs that were previously reported.

3.2. The Local Strain Distribution and Development During the In Situ Uniaxial Tensile Test

Fig. 2a–c shows the local strain distributions of the BAMCs measured by DIC at the strain of 6%. The tensile direction is parallel to the x direction. The micro-cracks formed in 3ABO and 5ABO during deformation are marked by yellow arrows in Fig. 2a–b, while the cracks in 10ABO are too small to observe. The crack total length was calculated by the accumulation of each crack length that perpendicular to tensile direction. Fig. 2d illustrates the development of crack total length and crack number in the BAMCs with increasing strain. The cracks in 5ABO nucleate more quickly than 3ABO due to its higher V_w. Besides, the value of crack length in 5ABO saturates at the strain of about 9% and keeps at a stable value, while that value in 3ABO saturates at a much higher strain of about 16%. It is noted that the higher the V_w, the denser and smaller the cracks in the BAMCs. The quantitative analysis of strain distribution was carried out and the standard deviation of strain (S) was utilized to evaluate the strain localization. The relationship between S and strain in the BAMCs is plotted in Fig. 2e. It is interesting that the

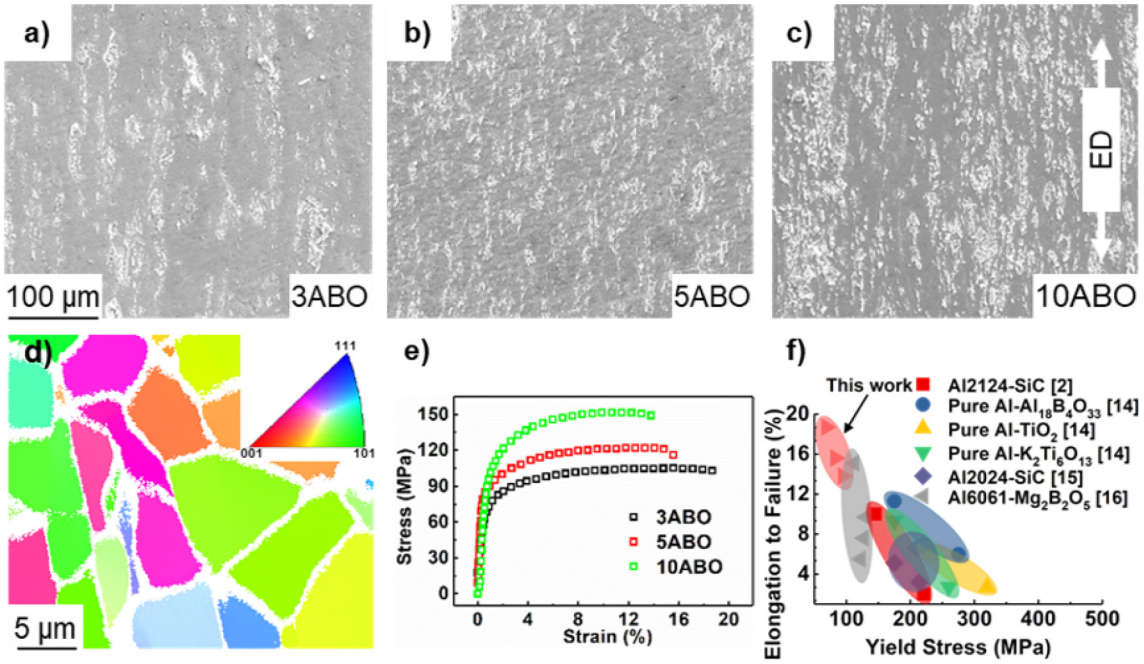

Fig. 1. The secondary electron micrographs of the as-annealed (a) 3ABO, (b) 5ABO and (c) 10ABO composites, respectively; (d) The EBSD IPF map of 10ABO composite; (e) The uniaxial tensile stress-strain curves of the BAMCs; (f) The summary of elongation to failure and yield stress for the AMCs from the present study and the literature.